SEISMIC AND WIND RISK EVALUATION OF REINFORCED CONCRETE TALL PIER BRIDGES LOCATED IN MOUNTAIN REGIONS

Aayush Aggarwal[1*], Swati Chaudhary[2]

[1]MTech in Structural Engineering, Department of Civil Engineering, Radha Govind Group of Institutions Meerut, Uttar Pradesh, Email ID: cpc.aayush@gmail.com*
[2]Associate Professor, Department of Civil Engineering, Radha Govind Group of Institutions, Meerut, Uttar Pradesh.

Corresponding Author:
Email ID: cpc.aayush@gmail.com

Abstract

The bridges built in the mountainous areas experience a combination of structural requirements because of the rocky terrain, high seismicity, and wind acceleration. This paper gives an account of an in-depth evaluation of a tall hollow circular reinforced concrete pier, 52.8 meters tall, supporting a highway bridge at the approach to the Khellani Tunnel in the Jammu and Kashmir region, which falls under the highest seismic risk category in India. The Indian Road Congress (IRC) design standards considered structural behavior under seismic and wind loading conditions using the numerical simulation tools, i.e., Structural Analysis and Design Program (STAAD Pro) and Midas Civil. It was found that the forces due to the wind, especially in the transverse direction, were greater than the seismic forces, and the highest wind force was recorded as 765.7 kilonewtons. This brings out wind as the controlling element in structural design in this case. The circular shape of the pier was hollow, which was determined to increase the performance due to the less mass of the structure, better lateral flexibility, and the ease of ductility. The building was able to achieve strength-based performance and serviceability-based performance requirements, and this shows that the design was compliant and resilient. The findings advocate for the wider adoption of hollow reinforced concrete piers in similar high-altitude, wind-sensitive regions. They also emphasize the importance of integrating wind considerations into seismic-resistant bridge design to ensure safety, economy, and long-term performance.

Keywords: Reinforced Concrete Pier, Seismic Vulnerability, Wind Analysis, Structural Analysis and Design Program, Hollow Section, Mountain Bridge

1. Introduction

Bridge construction is a crucial part of the process that is used to establish effective and reliable transportation systems (Yu, 2023). Tall Reinforced Concrete (RC) piers are one of the structural elements that determine the stability and resilience of bridges built in mountainous terrains. Such piers are frequently used as the foundation of bridge superstructures where the elevation differences caused by terrain require long spans and elevated roads (Zhou & Zhang, 2019). Tall piers facilitate the passage of difficult topographies by offering vertical clearance and structural continuity, and as such, they facilitate the growing infrastructural demands in high-altitude areas.

The technical and environmental complexities involved in the design and construction of tall piers in these areas are, however, not very easy. The mountainous areas, especially in the north of India, are in Zone V, which is an area with high-intensity ground motion risks. At the same time, the wind flows are increased in narrow valleys of these regions, which causes high lateral pressures on both superstructures and substructures (Li et al., 2024). Such dynamic forces necessitate that the bridge piers have not only strength but also ductility, flexibility, and energy-dissipating properties. In addition, their height-to-width ratios, foundation conditions, and slenderness bring in distinctive vulnerability patterns under seismic and wind loads (Su et al., 2021; Ye et al., 2022).

In the past, many bridge collapses in India have been related to the underestimation of such dynamic actions. According to Garg et al. (2022), in their extensive research on the bridge collapses between 1977 and 2017, they found that seismic shortcomings and wind-related instability were common phenomena, especially in hilly and riverine areas. Vibration due to wind, vortex shedding, and aerodynamic flutter may have a devastating effect on tall piers unless considered during the design stage (Kareem et al., 2019). Moreover, seismic areas in bridge networks experience downtimes after the event and cause transportation bottlenecks and economic losses (Zhang et al., 2023; Liu et al., 2022). Figure 1 indicates the destruction of highway bridges in the world by earthquakes since 2000.

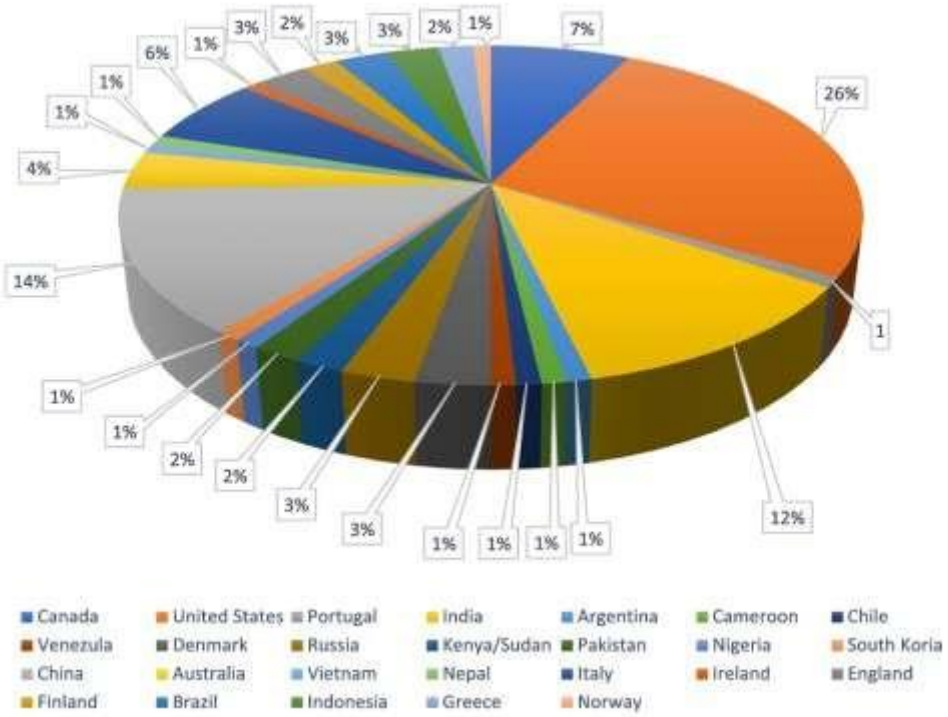

Figure 1 Country-wise bridge damages due to earthquakes from the year 2000 onwards (Thakkar et al., 2023

The Khellani Tunnel in the Union Territory of Jammu & Kashmir is such a high-risk area. The regional connectivity and military logistics rely on the infrastructure in this region, which is, however, vulnerable to chronic seismic and wind hazards. The object of the study is a steel composite girder bridge; the height of some of its piers is different, and the P1 pier is 52.8 meters high. This pier is circular in section and hollow, which implies that it has distinct structural properties that are beneficial and challenging in the lateral load situation. The hollow RC piers are commonly fevered due to the decreased seismic mass, ease of construction, and access to internal inspection, yet their performance has to be strictly evaluated under limit states (Jeswani & Budhlani, 2020; Falamarz-Sheikhabadi & Zerva, 2016).

In light of the context, this study seeks to conduct a comprehensive vulnerability analysis of the tall RC pier at the Khellani Tunnel bridge location. The main attention is paid to the quantification and comparison of the seismic and wind-induced loads on the structure, and then to the evaluation of its response and performance based on numerical modelling and codal compliance. The paper uses IRC SP:114-2018 as the seismic provisions and IRC:6-2017 as the wind loading requirements, which are the fundamental regulatory provisions in the design of Indian bridges. The structural analysis is performed with

the Structural Analysis and Design Program (STAAD.Pro), a popular structural engineering program that allows simulating a variety of load combinations and structural behavior of a structure at both elastic and ultimate limit states. The work is driven by a number of engineering objectives. To begin with, it aims at promoting the knowledge of the behavior of tall hollow piers subjected to simultaneous dynamic actions in complex terrain environments since the traditional design methods tend to treat seismic and wind loads separately (Joshi, 2023; Oppong et al., 2020). Second, it will optimize the hollow pier design to be efficient in the use of material and reinforcement, as well as structural integrity and serviceability. Remarkably, the confinement effects, reinforcement detailing, and pier slenderness are reviewed in terms of their impact on structural performance. Finally, the study strives to justify and generalize codal provisions to practical use by comparing the results of the analysis with IRC-compliant standards.

Moreover, the research will aim to become a part of the international debate about bridge weakness and strength, particularly concerning climate-related changes in wind patterns and the increasing urbanization of seismic regions (Thakkar et al., 2023; Srivastava et al., 2024). The interplay of bridge elements such as abutments, superstructure, and substructure also constitutes a key element of the vulnerability story (Kozak et al., 2018; Ma et al., 2024). Due to the emphasis on a practical case that has real implications, the results of the present work will help not only designers but also policymakers to improve the safety, sustainability, and flexibility of transport infrastructure in mountainous and hazard-prone areas.

This research has many objectives, which are aimed at improving the knowledge and strength of bridge structures in harsh conditions. To begin with, the proposed study will evaluate the structural behavior of the tall reinforced concrete hollow pier under the action of seismic and wind loads by means of analytical procedures. It also aims at determining the essential forces and possible failure modes through codal load combination and dynamic response behavior analysis. Moreover, the study aims at the optimization of the pier design to provide complete adherence to both Ultimate Limit State (ULS) and Serviceability Limit State (SLS) requirements. Besides, it examines the practical advantages and difficulties of the utilization of hollow circular reinforced concrete pier shapes, especially in the high-risk, mountainous regions. Finally, the research aims to contribute to the development of resilient bridge design systems, particularly in areas that are most vulnerable to seismic and wind-related risks.

2. Materials and Methods

2.1 Bridge and Site Description

The study focuses on the structural vulnerability assessment of a highway bridge located in the approach zone of the uni-directional Khellani Tunnel in the Union Territory of Jammu & Kashmir, a region categorized under seismic Zone V. This location presents complex topographic and environmental challenges, including steep gradients and intense lateral loads from both seismic and wind events. The bridge was designed to span a total length of 157.0 meters, subdivided into simply supported spans of 41.667 meters each, with a steel composite girder superstructure. Figure 2 indicates the general alignment and deck configuration and Figure 3 indicates the detailed geometry of the bridge at Pier P1.

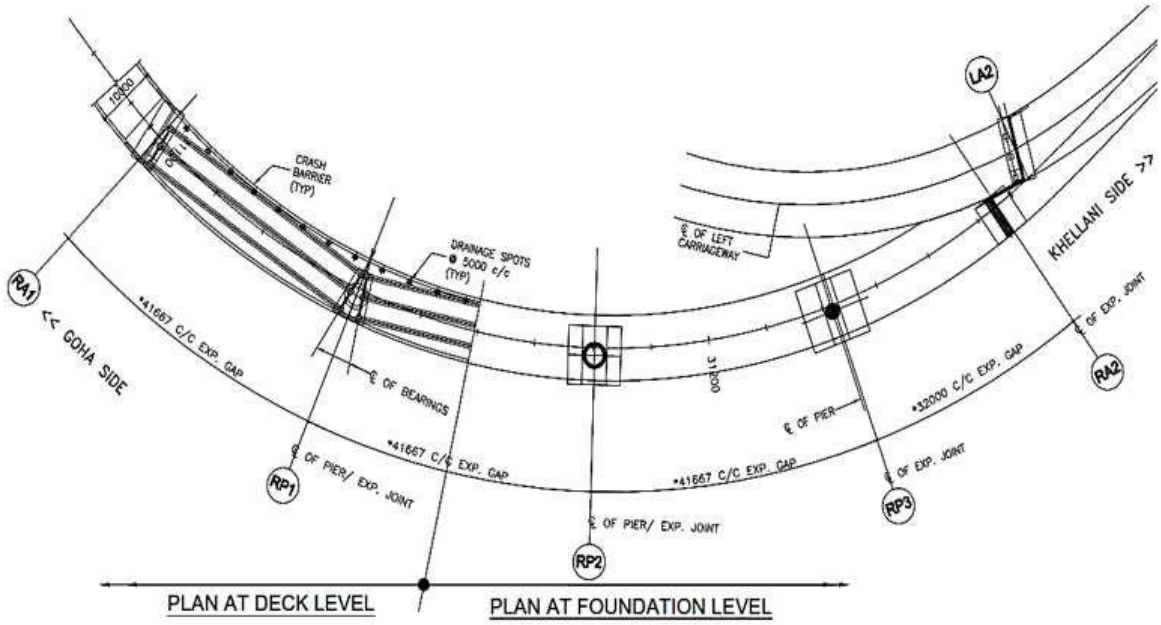

Figure 2: Plan showing horizontal alignment of the bridge

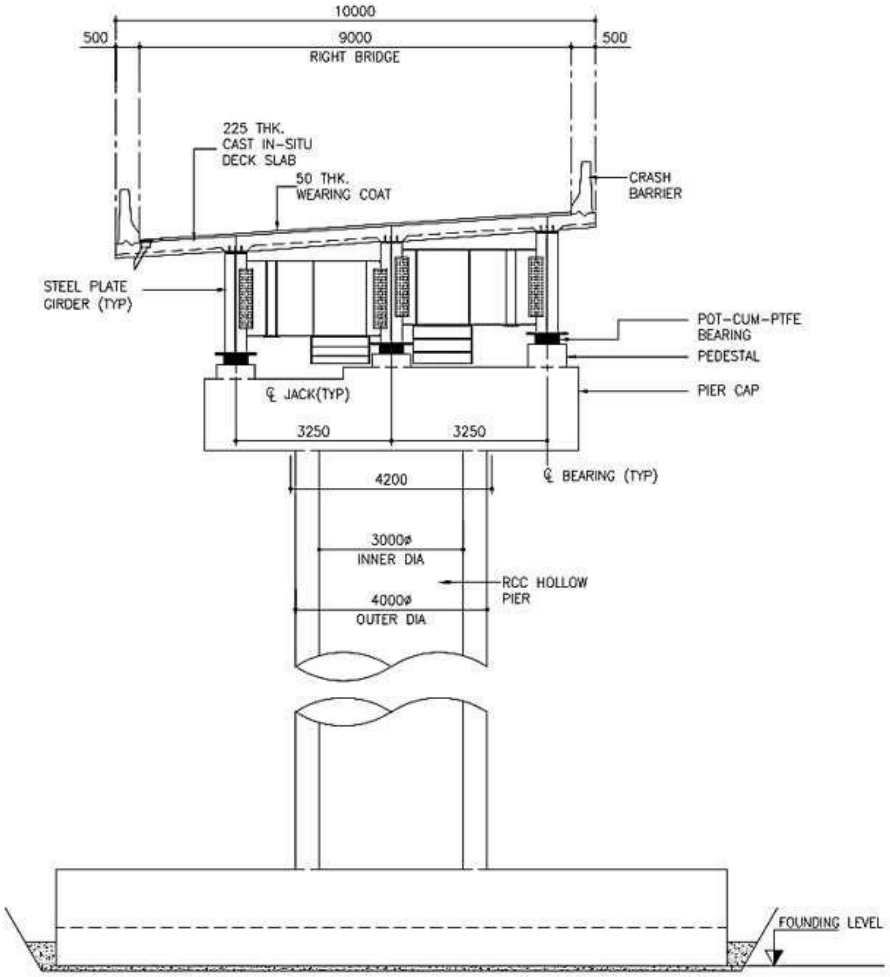

Figure 3: Cross-sectional view of bridge at pier P1

The primary structural element evaluated in this study was Pier P1, which exhibits the characteristics of a tall RC hollow circular pier. The pier stands 52.8 meters tall, with an external diameter of 4.0 meters and a wall thickness of 0.5 meters. This geometry not only aids in reducing the structural mass and enhancing ductility but also offers a favourable balance between material efficiency and seismic resistance. The pier carries a two-lane carriageway bridge deck of total width 10.0 meters, which includes a 225 mm thick deck slab and a 50 mm wearing course.
Foundation conditions include an open foundation system that is on moderately strong and slightly weathered rock strata. The reason this subsoil condition was selected was that it can support heavy vertical and lateral loads and has minimal settlement differences. The hollow section geometry and stable substrata increase the structural integrity and decrease seismic demand through the decrease in the centre of gravity and mass participation. The bridge layout, cross-sectional details, and pier arrangements were designed based on the existing Indian design specifications, keeping in view the site-specific loads and topographical limitations.

2.2 Analytical Tools and Codes

A structural analysis of the tall RC hollow pier under different loading conditions was performed to assess the structural response and performance of the tall RC hollow pier using STAAD Pro and Midas Civil, two popular Finite Element Analysis (FEA) software in bridge engineering.

2.2.1 Structural Modelling and Analysis Tools

- **STAAD Pro** was used for the primary structural modelling, especially to simulate linear static and dynamic behavior under different load combinations.
- **Midas Civil** was employed specifically for complex seismic evaluations, offering specialized capabilities for bridge pier and hydrodynamic response modelling.
- The two tools allowed incorporation of the design parameters according to applicable Indian codes and allowed simulation of actual load conditions, such as seismic and wind loads.
- **2.2.2 Applicable Design Standards and Load Considerations**
- The analysis was conducted in strict accordance with the following Indian design codes: Indian Road Congress Special (IRCSP) and Publication, and Indian Road Congress (IRC):
- **IRC SP:114-2018**: Guidelines for seismic design of highway bridges
- **IRC:6-2017**: Standard specifications for road bridges with emphasis on loads and load combinations

- **IRC:112-2020**: General features and design of concrete bridge components
- Load definitions included:
- **Dead Load (DL)**: Self-weight of structure and superimposed dead loads
- **Live Load (LL)**: Conforming to 70R wheeled and Class **A** vehicular loading
- **Seismic Load (SL)**: Based on Elastic Seismic Acceleration Method (ESAM) and Elastic Response Spectrum Method (ERSM)
- **Wind Load (WL)**: Evaluated per Clause 209 of IRC:6-2017
- **Hydrodynamic Forces**: Applied to submerged sections using the cylinder analogy method based on the seismic coefficient approach

Additional transient effects such as thermal loads, braking forces, and water current pressures were also considered for completeness, especially by Clauses 210.2 and relevant subclauses in IRC:6-2017 for pressure intensity and oblique flow conditions.

2.2.3 Seismic and Wind Analysis Techniques

In case of seismic vulnerability, both horizontal and vertical components of ground motion were considered. The seismic coefficient (ah) was derived based on the zone factor, importance factor, and response reduction factor, customized to suit the bridge type and pier configuration. The seismic demand was distributed along orthogonal axes as per the prescribed load combination rules outlined in IRC SP:114-2018.
Wind loads were assessed using:

- Basic wind speed maps
- Terrain categorization and topographical acceleration factors
- Hourly mean wind pressures
- Gust factors and drag/lift coefficients applicable to steel composite decks and pier sections

For superstructure design, wind loads were applied in transverse, longitudinal, and vertical directions simultaneously. Similarly, wind loads on substructure and live loads were computed using adjusted frontal areas and exposure conditions, particularly for a bridge height exceeding 50 meters.

2.2.4 Load Combinations

To ensure the structure's performance under real-world conditions, comprehensive load combinations were defined, including Ultimate Limit State (ULS) scenarios such as the sum of Dead Load (DL), Live Load (LL), and Wind Load (WL); Dead Load with half of the Live Load and Seismic Load (SL); and Dead Load, Live Load, Braking Force (BR), and Seismic Load. Additionally, Serviceability Limit State (SLS) combinations accounted for effects such as shrinkage, creep, and vibrations under frequent and quasi-permanent loading conditions.
Partial safety factors were applied per the provisions in Tables 1 and 2 of the IRC standards to address both strength verification and serviceability limits, thereby establishing a robust framework for evaluating structural performance.

Table 1: Partial Safety Factors for Verification of Structural Strength

Loads	Basic Combination	Accidental Combination	Seismic Combination
1. Permanent Loads			
1.1 Dead Load, Snow Load, SIDL (except surfacing)			
a) Adding to the effect of variable loads	1.35	1.0	1.35
b) Relieving the effect of variable loads	1.0	1.0	1.0
1.2 Surfacing			
a) Adding to the effect of variable loads	1.75	1.0	1.75
b) Relieving the effect of variable loads	1.0	1.0	1.0
1.3 Prestress and Secondary Effects of Prestress			
1.4 Backfill Weight			
a) When causing an adverse effect	1.35	1.0	1.0
b) When causing a relieving effect	1.0	1.0	1.0
1.5 Earth Pressure			
a) Adding to the effect of variable loads	1.5	1.0	1.0
b) Relieving the effect of variable loads	1.0	1.0	1.0
2. Variable Loads			
2.1 Carriageway Live Load, Braking, Tractive & Footway Live Load			
a) As leading load	1.5	0.75	-
b) As accompanying load	1.15	0.2	0.2
c) Construction Live Load	1.35	1.0	1.0
2.2 Wind Load (During Service and Construction)			
a) As leading load	1.5	-	-

b) As accompanying load	0.9	-	-
2.3 Live Load Surcharge (As accompanying load)	1.2	0.2	0.2
2.4 Construction Dead Load (e.g. launching girder, truss, etc.)	1.35	1.0	1.35
2.5 Thermal Loads			
a) As leading load	1.5	-	-
b) As accompanying load	0.9	0.5	0.5
3. Accidental Effects			
3.1 Vehicle Collision	-	1.0	-
3.2 Barge Impact / Floating Bodies	-	1.0	-
4. Seismic Effect			
a) During Service	-	-	1.5
b) During Construction	-	-	0.75

Table 2: Partial Safety Factors for Verification of Serviceability Limit State

Loads	**Rare Combination**	**Frequent Combination**	**Quasi-permanent Combination**
1. Permanent Loads			
1.1 Dead Load, Snow Load, SIDL (except surfacing & backfill weight)	1.0	1.0	1.0
1.2 Surfacing			
a) Adding to the effect of variable loads	1.2	1.2	1.2
b) Relieving the effect of variable loads	1.0	1.0	1.0
1.3 Earth Pressure	1.0	1.0	1.0
1.4 Prestress and Secondary Effect of Prestress			
1.5 Shrinkage and Creep Effect	1.0	1.0	1.0
2. Settlement Effects			
a) Adding to the permanent loads	1.0	1.0	1.0
b) Opposing the permanent loads	0	0	0
3. Variable Loads			
3.1 Carriageway Load (incl. braking, tractive, centrifugal) & Footway Live Load			
a) Leading Load	1.0	0.75	-
b) Accompanying Load	0.75	0.2	0
3.2 Thermal Load			
a) Leading Load	1.0	0.60	-
b) Accompanying Load	0.60	0.50	0.5
3.3 Wind Load			
a) Leading Load	1.0	0.60	-
b) Accompanying Load	0.60	0.50	0
3.4 Live Load Surcharge as Accompanying Load	0.80	0	0
4. Hydraulic Loads (Accompanying Loads)			
4.1 Water Current	1.0	1.0	-
4.2 Wave Pressure	1.0	1.0	-
4.3 Buoyancy	0.15	0.15	0.15

3. Results

3.1 Seismic Analysis

The seismic response of the tall RC hollow circular pier (Pier P1) was evaluated using both the Elastic Seismic Acceleration Method (ESAM) and the Elastic Response Spectrum Method (ERSM), in compliance with IRC: SP:114-2018. The analysis revealed a fundamental natural period of 2.368 seconds, indicating a highly flexible structure typical of tall piers with hollow sections. The increased time period contributes positively by reducing the spectral acceleration demand on the structure. Figure 4 shows the seismic zoning of India, placing the site in Zone V, confirming the critical seismic design requirement.

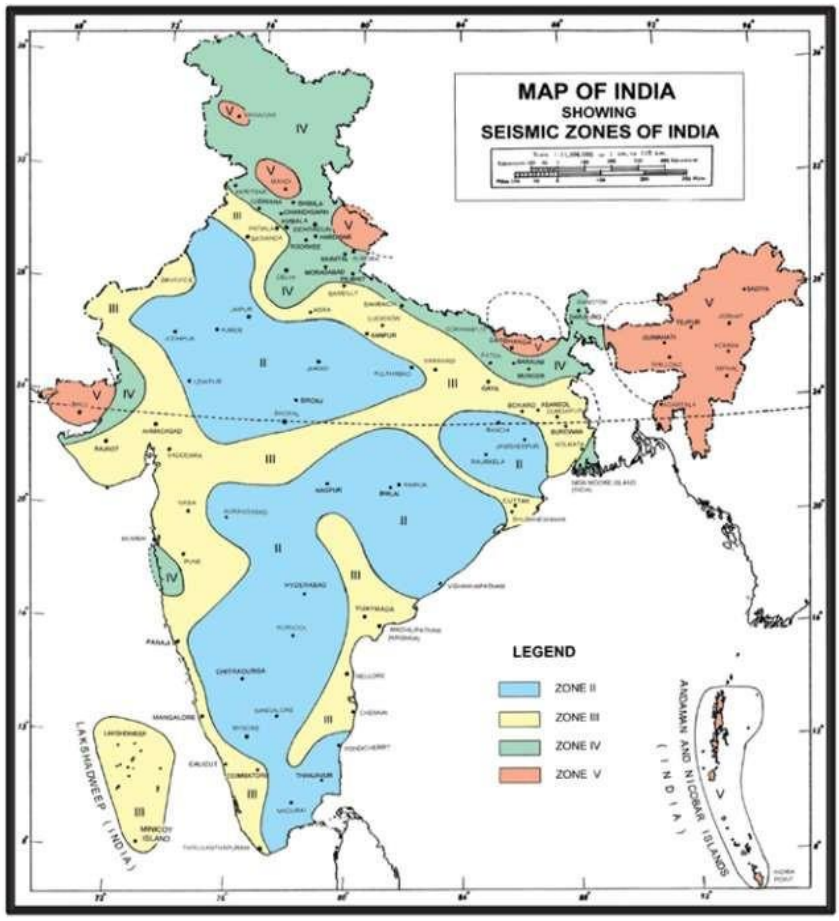

Figure 4: Seismic Zones in India

The base shear force and overturning moment values were derived from the dynamic analysis. For Design Basis Earthquake (DBE) conditions, the horizontal seismic coefficient (ah) was estimated at 0.065, while the vertical seismic coefficient (av) was 0.043. These coefficients, when applied with the pier's self-weight and live load contributions (as seismic mass), produced base shear forces and overturning moments within the permissible structural limits. Table 3 summarizes the response reduction factors used in the seismic load combinations as per codal specifications.

Table 3: Response Reduction Factor (R)

Bridge Component	**'R' with Ductile Detailing**
Substructure	
(i) Masonry / PCC Piers, Abutments	1.0
(ii) RCC Wall piers and abutments transverse direction (where plastic hinge cannot develop)	1.0
(iii) RCC Wall piers and abutments in longitudinal direction (where hinges can develop)	3.0
(iv) RCC Single Column	3.0
(v) RCC/PSC Frame (Refer Note VII)	3.0
(vi) Steel Framed	3.0
(vii) Steel Cantilever Pier	1.5
Bearings and Connections (see Note VI also)	1.0
Stoppers (Reaction Blocks) / Those restraining dislodgement or drifting away of bridge elements	1.0

A detailed distribution of internal forces across the pier height indicated peak shear and moment concentrations near the base, decreasing gradually along the shaft. The use of hollow cross-section contributed to a reduction in seismic mass, which in turn lowered the seismic demand. The flexibility offered by the pier also helped in absorbing ground motion without significant stress concentrations. Table 4 provides the zone factor (Z) relevant to the study area, contributing to the horizontal seismic coefficient.

Table 4: Zone Factor

Zone No.	Zone Factor (Z)
V	0.36
IV	0.24
III	0.16
II	0.10

3.2 Wind Load Results

Wind forces were computed as per IRC:6-2017, Clause 209, considering a basic wind speed of up to 47 m/s in the mountainous region near the Khellani Tunnel. The influence of complex terrain and valley-funnelling effects was accounted for by applying appropriate gust factors and terrain multipliers. Figure 5 illustrates the basic wind speed zones in India, with the study region falling in the 47 m/s zone.

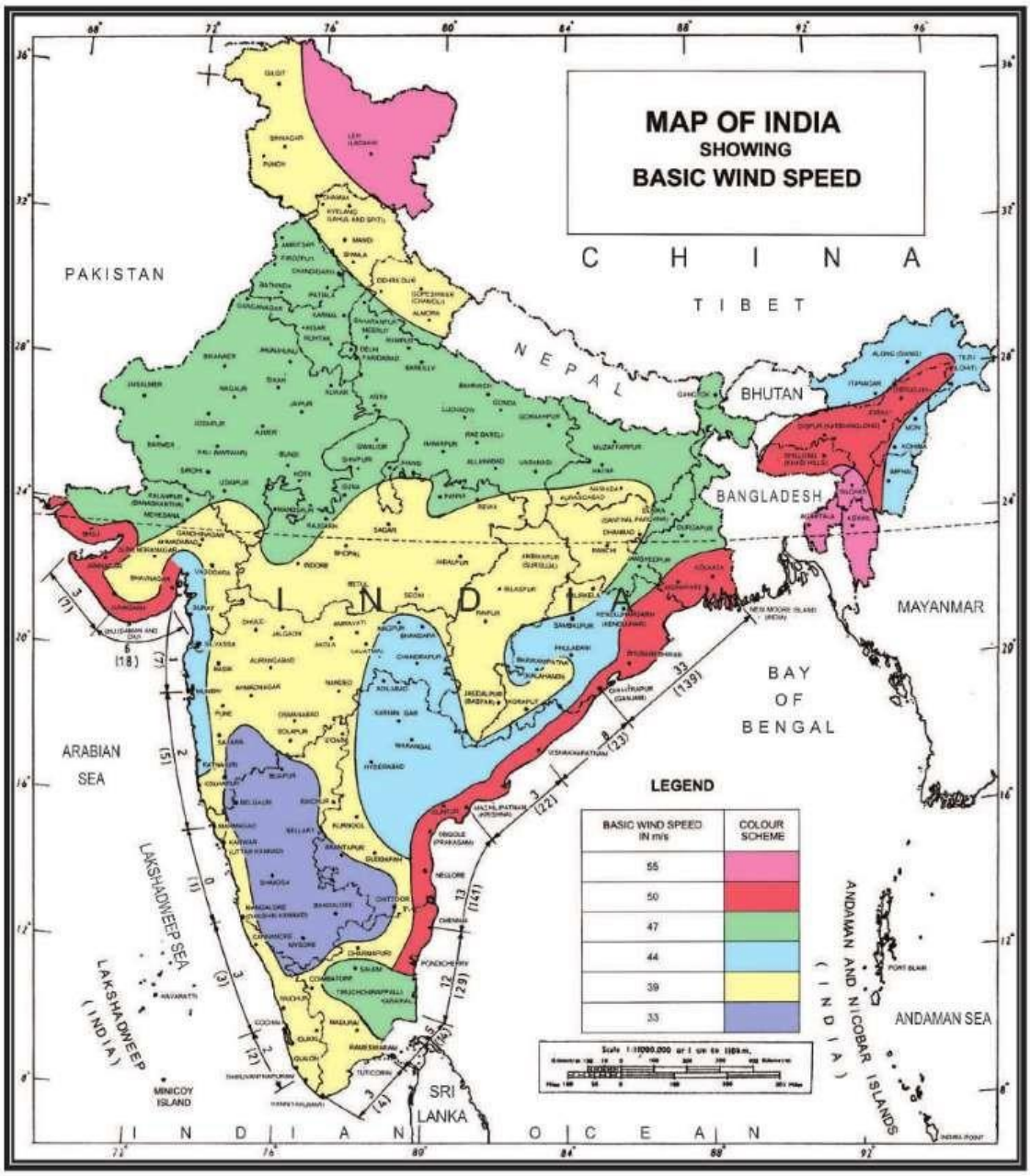

Figure 5: Basic Wind Speed in m/s (based on 50-years return period)

The calculated wind forces acting on the superstructure were found to be significant, with a transverse force of 765.7 kN, a vertical force of 583.8 kN, and a longitudinal force of 191.4 kN. For the substructure, which includes the tall pier P1, the corresponding forces were 364.0 kN in the transverse direction and 91.0 kN in the longitudinal direction. These results clearly indicate that wind loads exert a more critical influence than seismic loads, particularly on the steel composite girder and the tall piers. The lightweight nature of the steel girder makes it especially susceptible to uplift and lateral displacement under strong gusts, highlighting the importance of thoroughly evaluating aerodynamic stability and anchorage detailing. The superstructure was subjected to heightened aerodynamic demands, especially in the transverse direction, necessitating

the application of increased drag and lift coefficients during the design process. The aerodynamic response of the pier, owing to its hollow circular shape, proved advantageous by reducing drag effects through smoother flow paths around its surface.

3.3 Performance Evaluation

The structural performance of the pier was verified against both Ultimate Limit State (ULS) and Serviceability Limit State (SLS) criteria.

The design moment at the pier base under Ultimate Limit State (ULS) conditions was 10,347 kNm and the shear demands were in agreement with those of ESAM. The stresses in concrete and steel which were measured as 18.5 MPa and 275 MPa respectively were within the allowable design stresses and hence the utilization ratio was 0.959. This is an indication of effective utilization of structural materials. The circular geometry of the pier was hollow and this gave good lateral resistance and ductility to the pier which helped in the overall stability of the substructure.

The Serviceability Limit State (SLS) requirements were also met satisfactorily including such critical requirements as crack width control, deflection limits and long-term durability. The reinforcement detailing was well confined and aided these aspects as it enhanced the ductile response and strengthened the seismic resilience.

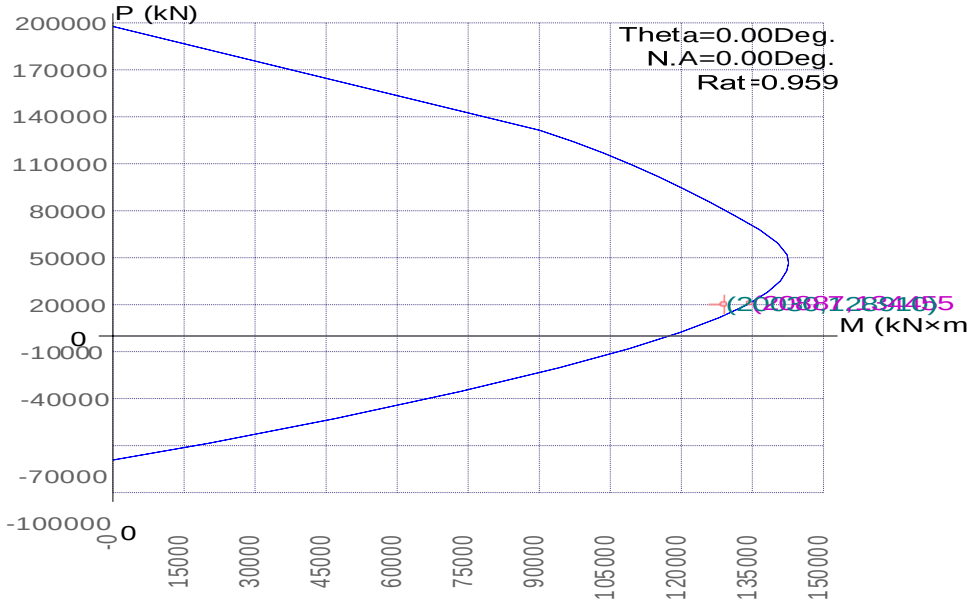

Figure 6: P-M graph under ULS load combination

Additional structural performance assessment under ULS and SLS was done using sophisticated sectional analysis and visual interpretation software. The axial force biaxial bending moment interaction surface shown in Figure 6 defines the full-strength envelope of the section and the red line is the actual loading path of combined seismic and service loading.

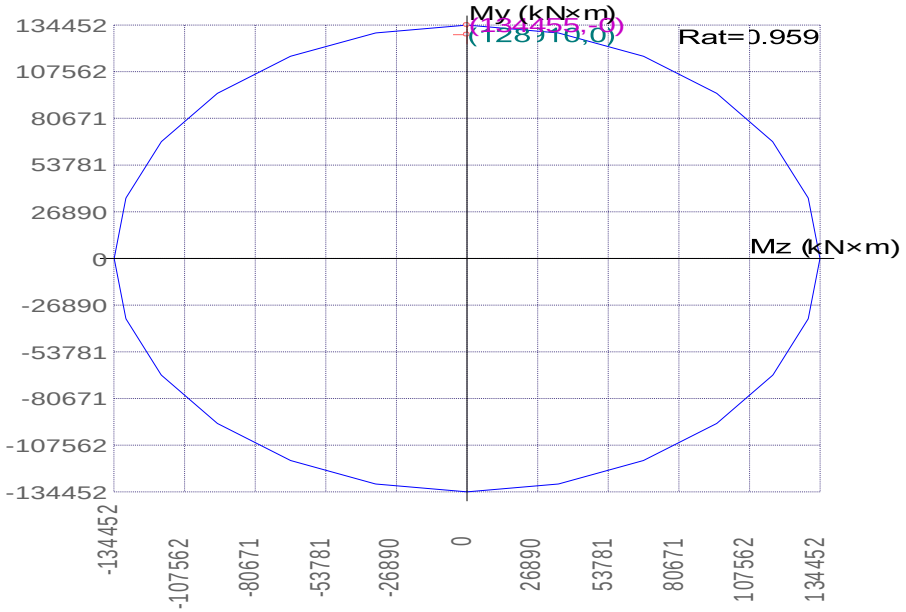

Figure 7: MY-MZ graph under ULS load combination

To complement this, the P-M interaction curve in two dimensions (Figure 7) shows the capacity of the axial load against the primary moment axis (My) and it is evident that the operational requirements are well within the section capacity.

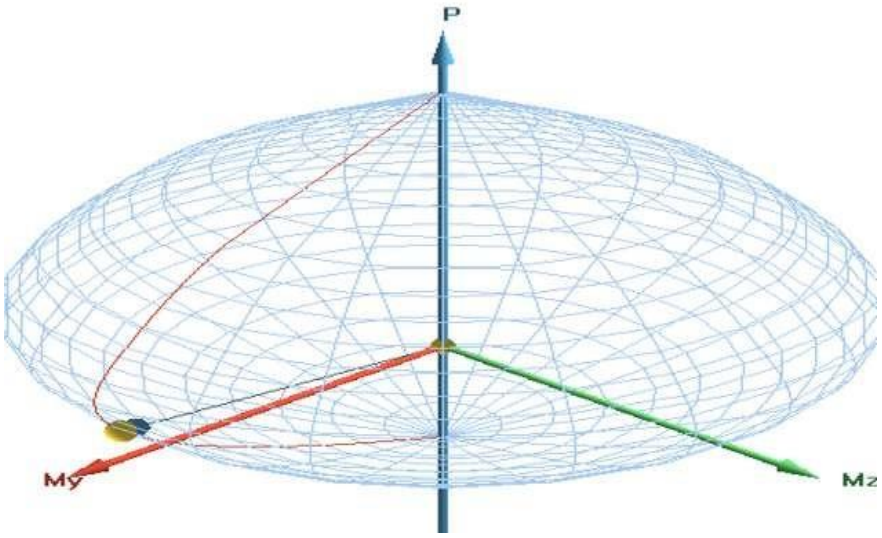

Figure 8: 3D interaction diagram for ULS load combination

The biaxial moment resistance (Mz vs My) is plotted on the moment interaction ellipse confirming the almost isotropic bending strength of the circular section (Figure 8), which is necessary in the case of multidirectional seismic loads.

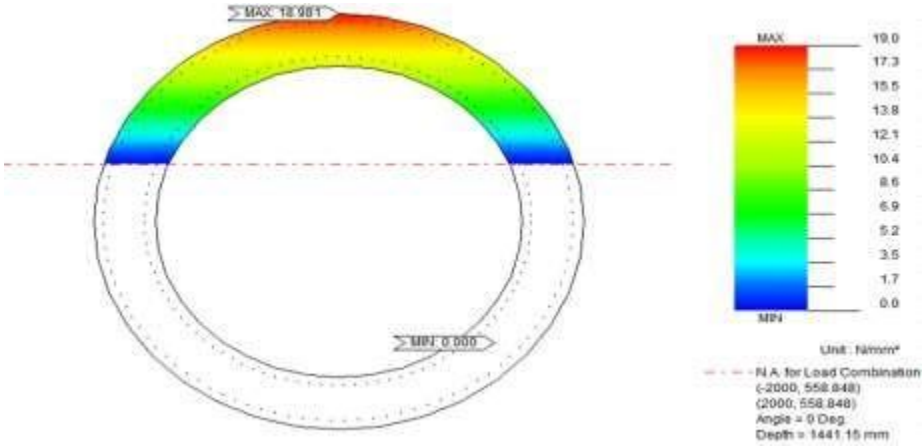

Figure 9: concrete stress values under SLS rare load combination (output from MIDAS GSD)

The elastic behavior of the pier is also depicted by stress distribution analysis under particular loading conditions. The contour of compressive stress (under load combination (2000, 558.848)) has the maximum values located at the upper face of the section shown in Figure 9.

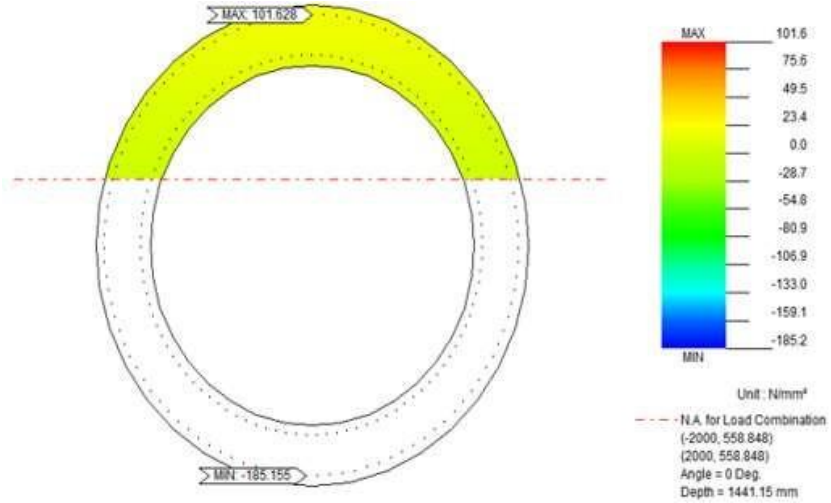

Figure 10: Reinforcement stress values under SLS rare load combination (output from MIDAS GSD)

The stress contour of load case (2000, 558.848) is in a reversed form where the lower half of the section is in tension and the upper half in compression shown in Figure 10. The structural symmetry and good stress transfer in the hollow circular geometry is evident in these plots and explains why it is appropriate in tall seismic-prone bridge piers.

Under Ultimate Limit State (ULS) conditions, the pier base experienced a design moment of 10,347 kNm, with shear demands aligned with ESAM-based values. Concrete and steel stresses (18.5 MPa and 275 MPa, respectively) remained within permissible limits, yielding a utilization ratio of 0.959, reflecting efficient material usage. The hollow circular pier provided effective lateral resistance and ductility. Serviceability Limit State (SLS) requirements were also met, including crack width, deflection, and durability, supported by well-confined reinforcement detailing that enhanced seismic resilience and overall structural performance.

4. Discussion

The structural evaluation of the RC hollow circular tall pier under both seismic and wind loading conditions yields critical insights into the performance of bridge elements in high-risk terrains such as the Himalayan belt. One of the central outcomes of this research is the clear dominance of wind loads over seismic loads in terms of force intensity and structural impact. This finding, while initially counterintuitive for a site located in Seismic Zone V, aligns with global research on bridge aerodynamics, which emphasizes that in narrow valleys or mountainous terrain, topographic acceleration of wind currents can produce highly amplified pressure zones (Kim et al., 2016; Chen et al., 2018). The wind pressure at the bridge site was nearly equal to a fundamental speed of 47 m/s and the resulting transverse, vertical and longitudinal forces were higher than the base shear calculated using seismic analysis.

The maximum transverse force of 765.7 kN, vertical uplift of 583.8 kN and longitudinal force of 191.4 kN were experienced in wind induced loading that posed higher lateral and vertical instability risks than the respective seismic coefficients (ah = 0.065; av = 0.043). These values are in line with the trends in the world where aerodynamic effects, such as buffeting, vortex shedding, and vibrations caused by wake have resulted in the redesign of similar structures (Li et al., 2021; Zhang et al., 2022). In conjunction with the wind tunnel tests, numerical assessment highlights the importance of the influence of wake effects and the surface flow separation as the dominant multipliers of the aerodynamic load in tall and flexible structures (Zhao et al., 2024; Ji et al., 2025).

Another interesting aspect that increases the structural performance of the pier is the use of hollow circular cross-section. The geometric structure has complex benefits: it minimizes seismic mass, allows internal inspection, enhances ductility under lateral forces, and has desirable aerodynamic characteristics because of the symmetry of the surface. The hollow pier is 52.8 meters tall, 4 meters in outer diameter and 0.5 meters in wall thickness, and was very useful in redistributing stress and dissipating energy throughout the structure. The lower self-weight, which did not sacrifice moment resistance, substantially reduced the seismic base shear, a characteristic that is consistent with the seismic design guidelines that should be applied to bridges with high piers in Zones IV and V (Liang et al., 2025).

The seismic resilience point of view also contributes to the performance of the pier as high-yield deformed reinforcement (Fe 550D) and M50-grade concrete are used to provide high flexural capacity and resistance to shear (Jara et al., 2015). The reinforcement detailing included confinement ties and transverse stirrups that are critical in ensuring the core integrity in the lateral deformation. This ductile detailing ensures that the pier remains in the elastic or mildly inelastic range under Design Basis Earthquake (DBE) events, thus conforming to the service life expectations outlined in IRC: SP:114-2018. The seismic analysis, utilizing both the Elastic Seismic Acceleration Method (ESAM) and the Elastic Response Spectrum Method (ERSM), confirmed that the fundamental period of 2.368 seconds results in a reduction of spectral acceleration. This response characteristic indicates that the structure avoids resonance with predominant ground motion frequencies, which often peak at around 0.5 to 1.5 seconds. The taller the structure and the longer the period, the less the force experienced due to resonance, assuming the structure remains within the DBE performance zone.

The comparative benefits of the hollow circular configuration, combined loading scenarios, such as seismic-wind interactions, must not be overlooked. The need to address multi-hazard loading is critical, particularly for bridges in remote, high-elevation regions that are susceptible to simultaneous extreme events, such as post-earthquake wind gusts or aftershock-induced soil softening (Liu et al., 2023). Research by Liang et al. (2025) demonstrates that under such compounded stress conditions, even resilient structures can exhibit high fragility indices unless reinforced with damping systems or designed with redundancy.

The current design, which adheres to Indian codal prescriptions (IRC:6-2017 and IRC: SP:114-2018), appears well-suited for Zone V environments. The ratio of utilization (0.959) and the acceptable stress levels (SLS) also prove that the structural design is efficient and compliant. To be reliable in the long-run, the future research should involve nonlinear time-history analysis and soil-structure interaction models particularly on piers that are more than 50 meters tall. In addition, it is worth paying more attention to aerodynamic instabilities such as buffeting and flutter, which are typical of long-span and tall-pier bridges. According to Zhang and Gruber (2020), biomimetic designs in nature, like vibration-tolerant structures, such as bamboo, may provide knowledge on how to improve resilience using form-based optimizations. Also, it is possible that future designs will incorporate active or passive damping systems, e.g. tuned mass dampers or base isolators, to reduce both the seismic and wind-induced response without unduly increasing structural stiffness or cost. This is a complete performance of this pier design and it represents a wider change in bridge engineering, a change that is shifting towards probabilistic and performance-based design philosophies. The resilience of modern infrastructure is being measured by the capacity of a structure to regain functionality after a disaster (Chen et al., 2017). The next step in high-performance bridge engineering will be to incorporate life-cycle cost analysis, downtime modeling and post-event retrofitting strategies into the initial design phase.

5. Conclusion

The paper provides an in-depth analysis of seismic and wind susceptibility of a tall hollow reinforced concrete pier that supports a highway bridge in the mountainous region of the Union Territory of Jammu and Kashmir, around the Khellani Tunnel.

Figure 11: Site image 1

Figure 12: Site image 2

Figures 11 and 12 present real construction photos of the viaduct piers located in the steep terrain close to the tunnel portal, which indicate the problematic site conditions that played an important role in the structural design decisions. The structure was evaluated with the help of sophisticated numerical tools under the Indian bridge design codes because it is located in an area that belongs to the highest seismic risk zone. It was found that wind loads, especially in the transverse direction, were more demanding on the structure than the seismic forces, because of topographic wind acceleration effects that are common in narrow valleys. The highest force due to wind was 765.7 kilonewtons, which was higher than the base shear due to seismic loading. The use of a hollow circular reinforced concrete pier was a major boost in terms of structural efficiency as it minimized seismic mass, increased ductility and maximized the use of materials. Structural performance checks showed that the structure satisfied all the design requirements under strength and serviceability-based conditions. The reinforcement detailing, confinement methods and the narrow geometry of the pier all worked in tandem to provide lateral stability and control of deformation of the pier. On the basis of these results, the study is very much in favor of the introduction of hollow circular piers in other high altitude and wind prone areas. Moreover, multi-hazard and dynamic simulation tools should be incorporated into the future design of bridges in these terrains to guarantee their structural safety, flexibility, and resilience in the long-term complex environmental conditions.

References

1. Chen, S., Zhou, Y., Wu, J., Chen, F., & Hou, G. (2017). Research of long-span bridges and traffic system subjected to winds: A system and multi-hazard perspective. *International journal of transportation science and technology*, *6*(3), 184-195.
2. Chen, Y., Dong, J., & Xu, T. (2018). Composite box girder with corrugated steel webs and trusses–A new type of bridge structure. *Engineering Structures*, *166*, 354-362.
3. Falamarz-Sheikhabadi, M. R., & Zerva, A. (2016). Effect of numerical soil-foundation-structure modeling on the seismic response of a tall bridge pier via pushover analysis. *Soil Dynamics and Earthquake Engineering*, *90*, 52-73.
4. Garg, R. K., Chandra, S., & Kumar, A. (2022). Analysis of bridge failures in India from 1977 to 2017. *Structure and Infrastructure Engineering*, *18*(3), 295-312.
5. Jara, J. M., Reynoso, J. R., Olmos, B. A., & Jara, M. (2015). Expected seismic performance of irregular medium-span simply supported bridges on soft and hard soils. *Engineering Structures*, *98*, 174-185.
6. Jeswani, B., & Budhlani, D. (2020). A review paper on analysis and design of bridge components using Staad Pro. *Int Res J Eng Technol*, *7*, 4707-4709.
7. Ji, C., Leng, S., Townsend, J. F., Mei, D., & Xu, G. (2025, June). Stochastic dynamic response of a sea-crossing suspension bridge with a span over 2000m subject to coupled wind–wave action. In *Structures* (Vol. 76, p. 108830). Elsevier.
8. Joshi, S. (2023). Recent Enhancement of Indian Bridge Management System. *Structural Engineering International*, *33*(2), 283-290.
9. Kareem, A., Hu, L., Guo, Y., & Kwon, D. K. (2019). Generalized wind loading chain: Time-frequency modeling framework for nonstationary wind effects on structures. *Journal of Structural Engineering*, *145*(10), 04019092.
10. Kim, S. J., Yoo, C. H., & Kim, H. K. (2016). Vulnerability assessment for the hazards of crosswinds when vehicles cross a bridge deck. *Journal of Wind Engineering and Industrial Aerodynamics*, *156*, 62-71.
11. Kozak, D. L., LaFave, J. M., & Fahnestock, L. A. (2018). Seismic modeling of integral abutment bridges in Illinois. *Engineering Structures*, *165*, 170-183.
12. Li, S., Li, Q., Guo, P., Liu, X., Wang, D., & Wang, X. (2021, August). Wake-induced vibrations of iced pin joint hangers of suspension bridges based on wind tunnel test and new method of transiting test. In *Structures* (Vol. 32, pp. 588-603). Elsevier.
13. Li, W., Cui, S., Zhao, J., An, L., Yu, C., Ding, Y., ... & Liu, Q. (2024). Experimental Study of Wind Characteristics at a Bridge Site in Mountain Valley Considering the Effect of Oncoming Wind Speed. *Applied Sciences*, *14*(22), 10588.
14. Liang, Y., Zhao, T., Wei, Y., & Guan, P. (2025). Fragility analysis of cross-sea highway cable-stayed bridges under seismic-wind combined loading. *Engineering Failure Analysis*, *173*, 109451.
15. Liu, Z., Li, S., Zhao, W., & Guo, A. (2022). Post-earthquake assessment model for highway bridge networks considering traffic congestion due to earthquake-induced bridge damage. *Engineering Structures*, *262*, 114395.
16. Liu, Z., Liu, J., Yan, J., Guo, A., & Li, H. (2023). Dynamic responses of the end-anchored floating bridge under the combined action of wind and waves. *Ocean Engineering*, *288*, 115907.
17. Ma, L., Li, Z., Xu, H., & Cai, C. S. (2024). Numerical study on the dynamic amplification factors of highway continuous beam bridges under the action of vehicle fleets. *Engineering Structures*, *304*, 117638.
18. Oppong, K., Saini, D., & Shafei, B. (2020). Vulnerability assessment of bridge piers damaged in barge collision to subsequent hurricane events. *Journal of Bridge Engineering*, *25*(8), 04020051.
19. Srivastava, C., Pandikkadavath, M. S., Mangalathu, S., & AlHamaydeh, M. (2024, March). Seismic response of RC bridges under near-fault ground motions: A parametric investigation. In *Structures* (Vol. 61, p. 106033). Elsevier.
20. Su, J., Li, Z. X., Dhakal, R. P., Li, C., & Wang, F. (2021, February). Comparative study on seismic vulnerability of RC bridge piers reinforced with normal and high-strength steel bars. In *Structures* (Vol. 29, pp. 1562-1581). Elsevier.
21. Thakkar, K., Rana, A., & Goyal, H. (2023). Fragility analysis of bridge structures: a global perspective & critical review of past & present trends. *Advances in Bridge Engineering*, *4*(1), 10.
22. Ye, L., Wang, Y., & Xie, W. (2022, November). Seismic fragility and loss assessment on earthquake-resilient double-column tall piers with shear links subjected to far-field and near-fault ground motions. In *Structures* (Vol. 45, pp. 1774-1787). Elsevier.
23. Yu, J. (2023). The Bridge Type Quadrant Diagram and New Basic Bridge Type: Umbrella Truss Bridge. Pre-stress Technology, 3, 15-29.
24. Zhang, M., Zhang, J., Long, J., Li, Y., Zou, Y., & Yin, D. (2022). CFD Numerical simulation of wind field and vehicle aerodynamic characteristics on truss bridge deck under crosswind. *KSCE Journal of Civil Engineering*, *26*(12), 5146-5159.
25. Zhang, W., & Gruber, P. (2020). Wind-resilient civil structures: what can we learn from nature. *Botany*, *98*(1), 37-48.
26. Zhang, Z., Ji, T., & Wei, H. H. (2023). Assessment of post-earthquake resilience of highway–bridge networks by considering downtime due to interaction of parallel restoration actions. *Structure and Infrastructure Engineering*, *19*(5), 589-605.
27. Zhao, L., Wang, Z., Chen, W., & Cui, W. (2024). Buffeting performance of long-span bridges with different span affected by parametric typhoon wind. *Journal of Wind Engineering and Industrial Aerodynamics*, *254*, 105903.
28. Zhou, X., & Zhang, X. (2019). Thoughts on the development of bridge technology in China. *Engineering*, *5*(6), 1120-1130.